Microbial Physiology

Research Article

Microb Physiol 2022;32:71–82
DOI: 10.1159/000521970

Received: August 19, 2021
Accepted: January 12, 2022
Published online: February 15, 2022

Migration of Polyphosphate Granules in *Agrobacterium tumefaciens*

Celina Frank[a] Daniel Pfeiffer[b] Meriyem Aktas[c] Dieter Jendrossek[a]

[a]Institute of Microbiology, University of Stuttgart, Stuttgart, Germany; [b]Department of Microbiology, University Bayreuth, Bayreuth, Germany; [c]Microbial Biology, Ruhr University Bochum, Bochum, Germany

Keywords
Polyphosphate · Polyphosphate kinase · Polyphosphatosome

Abstract
Agrobacterium tumefaciens has two polyphosphate (polyP) kinases, one of which ($PPK1_{AT}$) is responsible for the formation of polyP granules, while the other ($PPK2_{AT}$) is used for replenishing the NTP pools by using polyP as a phosphate donor to phosphorylate nucleoside diphosphates. Fusions of eYFP with $PPK2_{AT}$ or of the polyP granule-associated phosin PptA from *Ralstonia eutropha* always co-localized with polyP granules in *A. tumefaciens* and allowed the tracking of polyP granules in time-lapse microscopy experiments without the necessity to label the cells with the toxic dye DAPI. Fusions of $PPK1_{AT}$ with mCherry formed fluorescent signals often attached to, but not completely co-localizing with, polyP granules in wild-type cells. Time-lapse microscopy revealed that polyP granules in about one-third of a cell population migrated from the old pole to the new cell pole shortly before or during cell division. Many cells de novo formed a second (nonmigrating) polyP granule at the opposite cell pole before cell division was completed, resulting in two daughter cells each having a polyP granule at the old pole after septum formation. Migration of polyP granules was disordered in mitomycin C-treated or in PopZ-depleted cells, suggesting that polyP granules can associate with DNA or with other molecules that are segregated during the cell cycle.

Introduction

The formation of polyphosphate (polyP) granules (also designated as volutin granules) in microorganisms has been known for more than a hundred years [Meyer, 1904; Harold, 1966]. In prokaryotes, polyP is formed as globular inclusions with diameters mostly in the range from 50 to ≈200 nm (recently reviewed in [Jendrossek, 2020]). PolyP granules are reservoirs of phosphorous and (divalent) cations but can have several other functions, e.g., resistance to various forms of stresses (for reviews see [Kornberg et al., 1999; Rao et al., 2009]). Recent studies in *Ralstonia eutropha* (also *Cupriavidus necator*) showed that several proteins, including polyP kinases (PPKs) [Tumlirsch et al., 2015], phosins (proteins with

Karger@karger.com
www.karger.com/mip

Correspondence to:
Dieter Jendrossek, dieter.jendrossek@imb.uni-stuttgart.de

CHAD-motifs such as PptA or PptB) [Tumlirsch and Jendrossek, 2017], and others, are specifically attached to polyP granules in vivo, suggesting that polyP granules are supramolecular complexes for which the designation as polyphosphatosomes has been proposed [Jendrossek, 2020]. Only little attention has been paid, however, to the question whether the localization of polyP granules (in prokaryotes) is random or is a controlled process. In cyanobacteria, *Synechococcus elongatus*, for example, a specific positioning system (McdA and McdB) has been recently discovered that determines the equidistant positioning of carboxysomes in the nucleoid region [MacCready et al., 2018; MacCready et al., 2020]. In *Magnetospirillum gryphiswaldense*, the positioning of the magnetosome chain in the middle of the spirillum-shaped cells depends on a magnetosome-specific cytoskeleton (MamK and MamJ) including an active repositioning of the split magnetosome chain system after cell division [Toro-Nahuelpan et al., 2016]. The finding that the positioning of several organelle-like structures is actively controlled suggests that the positioning of polyP granules (polyphosphatosomes) might be also controlled by the cell. In a few publications, polyP granules were found located in or associated with the nucleoid region of *Myxococcus xanthus* [Voelz et al., 1966], *Pseudomonas aeruginosa* [Takade et al., 1991; Racki et al., 2017], *Caulobacter crescentus* [Henry and Crosson, 2013], *R. eutropha* [Tumlirsch et al., 2015], or *S. elongatus* [Murata et al., 2016], but specific target molecules or target structures, which polyP granules might interact with or bind to, have not been identified.

In contrast to the specific localization of polyP granules in the nucleoid region, polyP granules in some bacterial species are specifically localized in the cell pole region: *Corynebacterium glutamicum*, for example, forms two polyP granules, one at each cell pole [Pallerla et al., 2005]. A similar observation was made in *Agrobacterium tumefaciens*, a species with a polar growth mode [Brown et al., 2012]. Most *A. tumefaciens* cells formed one polyP granule that was generally located near one of the cell poles [Seufferheld et al., 2003; Frank and Jendrossek, 2020]. Due to the impact of the polar growth mode on cell polarity in *A. tumefaciens*, we wondered whether the polyP granule is located at the growth pole (GP) or at the old cell pole (OP) and what happens if the GP switches to an OP after cell division. To our surprise, we observed that the polyP granules in some cells migrated from the OP to the upcoming new GP of the cell during the process of cell growth and cell division. To our knowledge, a subcellular microscopically trackable migration of organelle-like supramolecular complexes has been so far described only for the magnetosome chain, which is repositioned from the new cell poles to mid-cell after cell division in *M. gryphiswaldense* [Toro-Nahuelpan et al., 2016].

Results and Discussion

$PPK2_{AT}$ Is Always Attached to polyP Granules

Plasmid-derived expression of an *eyfp-$ppk2_{AT}$* fusion (or *mCherry-$ppk2_{AT}$*) in *A. tumefaciens* resulted in the formation of cell pole-localized fluorescent foci. Cells had either one, two, or – rarely – three eYFP-$PPK2_{AT}$ (or mCherry-$PPK2_{AT}$) foci. Staining of the cells with DAPI and imaging at a DAPI-polyP-specific wavelength revealed that 70%, 29%, and 0.8% of the cells had one, two, or three polyP granules, respectively, that always co-localized with eYFP-$PPK2_{AT}$ (or mCherry-$PPK2_{AT}$) foci (online suppl. Fig. s1a, b, f; for all online suppl. material, see www.karger.com/doi/10.1159/000521970). We never detected a DAPI-polyP signal without an eYFP-$PPK2_{AT}$ focus. This confirmed our previous observation that $PPK2_{AT}$ of *A. tumefaciens* is a polyP-associated protein and that expression of *eyfp-$ppk2_{AT}$* is a suitable tool to monitor the formation and the localization of polyP granules. The same result was obtained when a fusion of the *eyfp* gene with the gene coding for the CHAD domain-containing phosin protein PptA of *R. eutropha* [Tumlirsch and Jendrossek, 2017] was expressed in *A. tumefaciens* (online suppl. Fig. s1c). The eYFP-$PptA_{RE}$ fusion always co-localized with polyP granules and confirmed the in vitro binding of phosins to polyP [Lorenzo-Orts et al., 2019; Werten et al., 2019] also in vivo. Thus, the monitoring of eYFP-$PPK2_{AT}$ or eYFP-$PptA_{RE}$ allowed us to follow the polyP granule localization in living cells in time-lapse experiments by avoiding staining of the cells with the toxic dye DAPI.

No eYFP-$PPK2_{AT}$ foci (or mCherry-$PPK2_{AT}$ foci or eYFP-$PptA_{RE}$) were detected when *eyfp-$ppk2_{AT}$* (or *mCherry-$ppk2_{AT}$* or *eyfp-$pptA_{RE}$*) was expressed in a polyP-free *A. tumefaciens* background (*$\Delta ppk1_{AT}\Delta ppk2_{AT}$* mutant). Instead, fluorescence of eYFP-$PPK2_{AT}$ (or mCherry-$PPK2_{AT}$ or eYFP-$PptA_{RE}$) was dispersed throughout the cell and staining of these cells with DAPI confirmed the absence of DAPI-polyP-specific foci (online suppl. Fig. s1d, e). This result is in agreement with our previous observation that $PPK2_{AT}$ does not catalyze the formation of polyP in vivo in *A. tumefaciens* and suggests that $PPK2_{AT}$ of *A. tumefaciens* is important for replenishing NTP pools at the expense of previously accumulated polyP [Frank et al., 2020].

Cells with only a single polyP granule generally had this polyP granule located at the OP as confirmed by co-expression of an *eyfp-popZ* fusion in combination with DAPI-polyP staining. PopZ is a pole-organizing protein well-known in alpha-proteobacteria [Bowman et al., 2008; Ebersbach et al., 2008; Grangeon et al., 2015; Pfeiffer et al., 2019], and $PopZ_{AT}$-eYFP in growing cells is located at the GP. Consequently, $PopZ_{AT}$-eYFP foci and DAPI-polyP foci were located at opposite cell poles (online suppl. Fig. s2). Cells with more than one polyP granule never had two granules at/near the same cell pole. Instead, most cells with two polyP granules had one polyP granule at each cell pole, and only occasionally we detected cells with one polyP granule at a cell pole and a second polyP granule somewhere between the cell poles (online suppl. Fig. s3). Figure 1 shows a graphic representation of the distance from the OP of 257 eYFP-$PPK2_{AT}$ foci representing 257 polyP granules in relation to cell length. It is evident that short cells (<3.5 µm) mainly had only one polyP granule that was located near the OP. By contrast, longer cells with >3.5 µm length had either one or two polyP granules. In the majority of the cells with two polyP granules, these polyP granules were located at each of the cell poles (83%), and only a minor fraction (17%) had one polyP granule between the cell poles. Since larger cells are in a later stage of the cell cycle compared to short cells, the frequent detection of two polyP granules in long cells suggests that new polyP granules are formed at the GP, thus explaining the general localization of one polyP granule at the OP in freshly divided (short) cells.

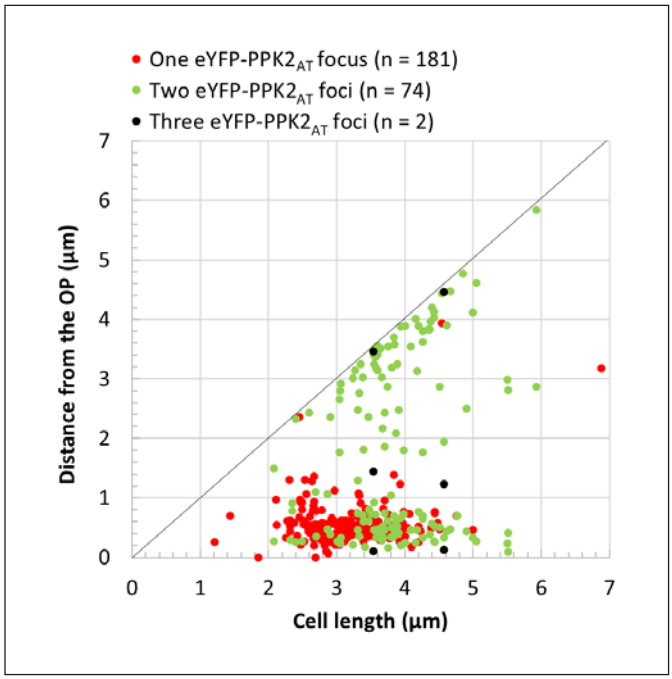

Fig. 1. Dependence of polyP granule localization on cell length. The positions of polyP granules were determined in FM1-43-stained *A. tumefaciens* cells harboring pBBR1MCS2-*eyfp-ppk2*$_{AT}$ and were plotted against cell lengths. FM1-43 preferentially stains the OP [Zupan et al., 2013].

$PPK1_{AT}$ Is Closely Associated with Formed polyP Granules

A. tumefaciens mutants with deletion of *ppk1*$_{AT}$ or of both *ppk1*$_{AT}$ and *ppk2*$_{AT}$ (but not with a deletion of *ppk2*$_{AT}$ only) are deficient in polyP granule formation. Therefore, only $PPK1_{AT}$ is essential and responsible for polyP formation in *A. tumefaciens*. To monitor the subcellular localization of $PPK1_{AT}$, we expressed fusions of *mCherry* with the *ppk1*$_{AT}$ gene in *A. tumefaciens*, which generally led to single fluorescence foci. When *ppk1*$_{AT}$-*mCherry* was expressed in a wild-type background, the fluorescence signals were almost exclusively located at the GP (Fig. 2a, black dots), suggesting that this is the location from where polyP granules originate. Remarkably, an inactive form of $PPK1_{AT}$, in which the active site (H450) had been replaced by an alanine [$PPK1_{AT}$(H450A)-mCherry variant], localized mainly (≈89%) at or near the OP and was detected only in about 11% of all cases at the GP (Fig. 2a, green dots). In the absence of polyP, i.e., in a *Δppk1*$_{AT}$, *Δppk2*$_{AT}$ background, PPK1(H450A)-mCherry foci were detected not only at the poles but also throughout the cells (Fig. 2b, orange dots). This result means that foci formation of $PPK1_{AT}$(H450A)-mCherry is an intrinsic property of the enzyme and does not depend on the presence of polyP granules. This is in contrast to $PPK2_{AT}$, which is soluble in a polyP-deficient (*Δppk1*$_{AT}$) background. Apparently, the correct localization of $PPK1_{AT}$ requires a catalytically active enzyme and/or the presence of polyP granules. A similar observation of a mis-localized PPK1 has been previously described for an inactive Venus-PPK1(H434A) variant in *C. crescentus* [Henry and Crosson, 2013]. The detection of about 11% of correctly (at the GP) localized $PPK1_{AT}$(H450A)-mCherry foci in a wild-type background might be explained by hetero-oligomer formation of active $PPK1_{AT}$-mCherry monomers with inactive $PPK1_{AT}$(H450A)-mCherry monomers. The reason why $PPK1_{AT}$-mCherry foci in the *Δppk1*$_{AT}$, *Δppk2*$_{AT}$ background were detected mainly (75%) at the OP and only rarely (24%) at the GP (Fig. 2b, blue dots) remains unclear.

Microb Physiol 2022;32:71–82
DOI: 10.1159/000521970

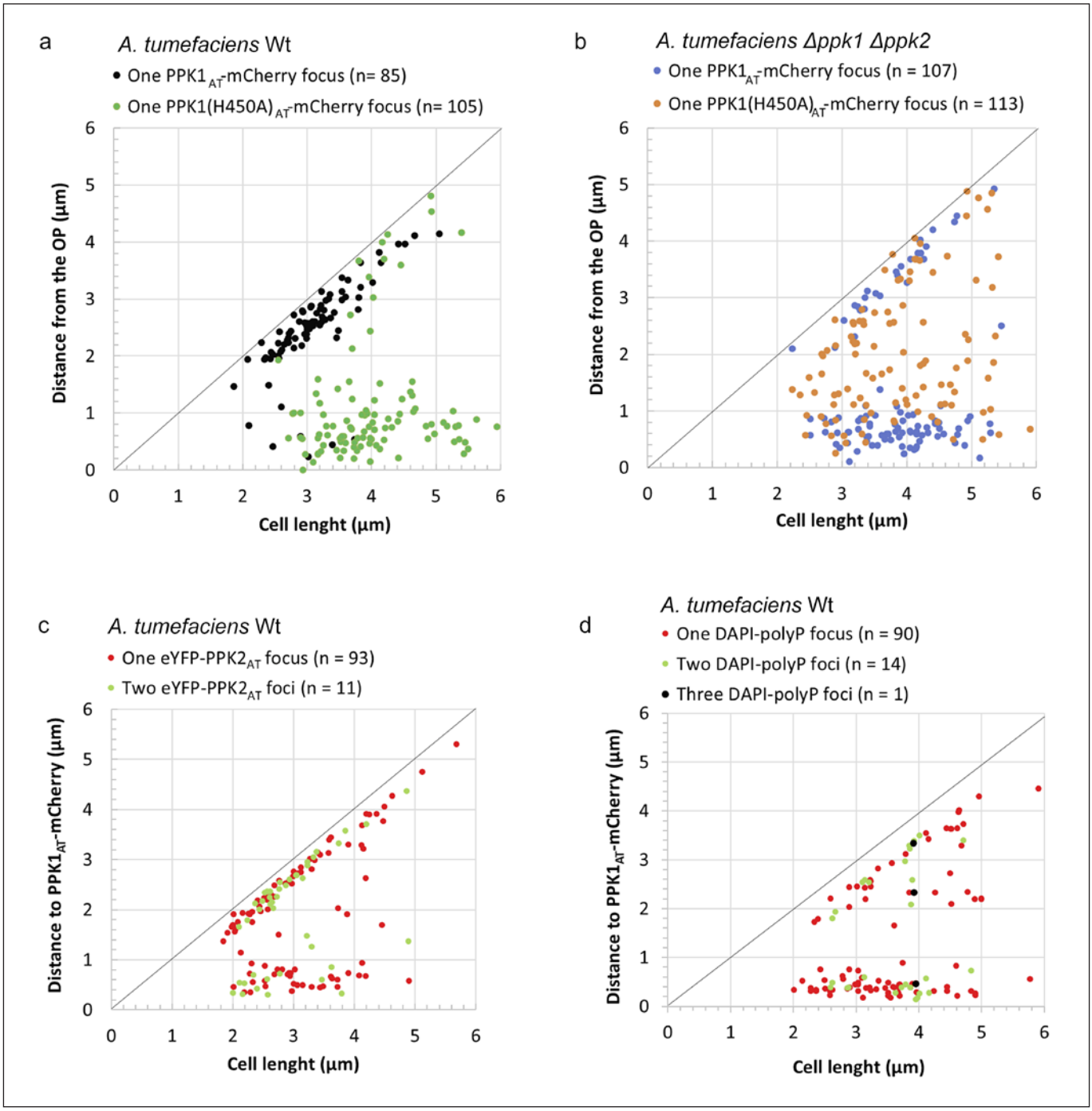

Fig. 2. Localization of $PPK1_{AT}$-mCherry variants and polyP granules. The positions of wild-type $PPK1_{AT}$-mCherry foci and inactive $PPK1_{AT}$(H450A)-mCherry foci relative to the OP in *A. tumefaciens* backgrounds as indicated are shown in (**a**) and (**b**), respectively. The distances of polyP granules detected in the form of eYFP-$PPK2_{AT}$ foci (**c**) or DAPI-polyP foci (**d**) relative to $PPK1_{AT}$-mCherry foci at the GP are shown in (**c**) and (**d**). The position of the highest fluorescence intensity of the elongated $PPK1_{AT}$-mCherry foci or $PPK1_{AT}$(H450A)-mCherry foci were taken for determination of intracellular distances. All strains were grown in lysogeny broth medium.

Microb Physiol 2022;32:71–82
DOI: 10.1159/000521970

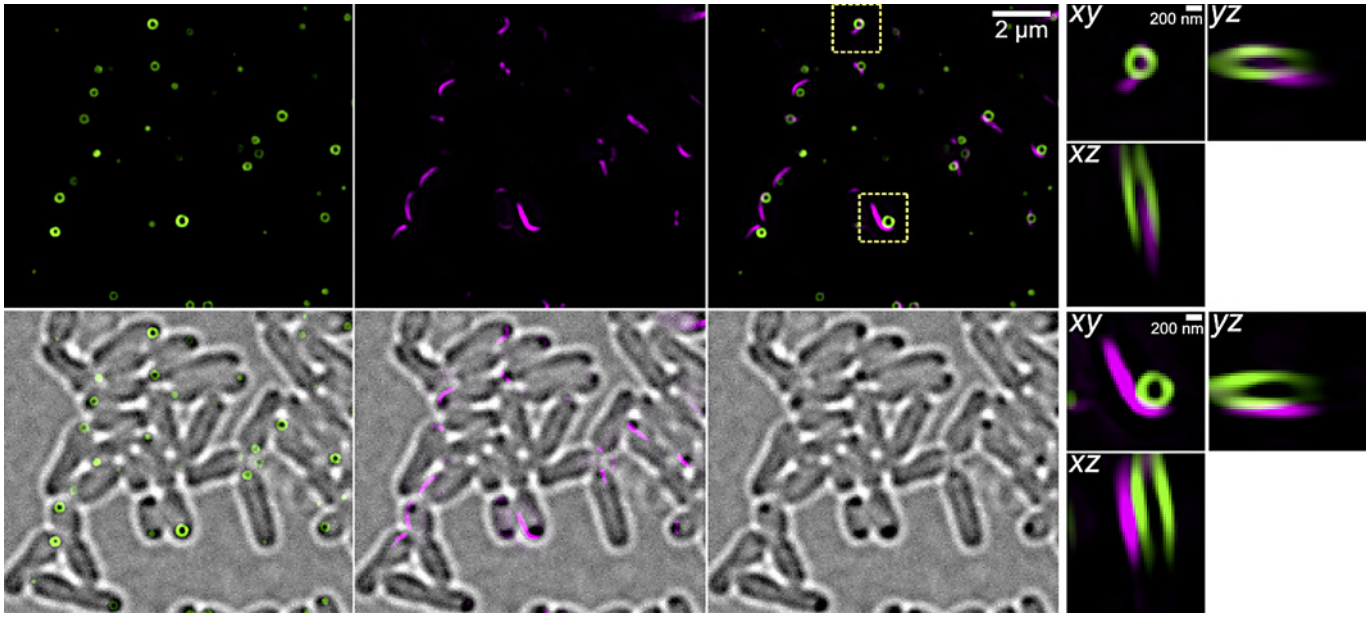

Fig. 3. Three-dimensional structured illumination microscopy (3D-SIM) of *A. tumefaciens*. *A. tumefaciens* wild-type cells harboring pBBR1MCS2-*ppk1*$_{AT}$-*mCherry* and pTrc200-P$_{lac}$-*eyfp-ppk2*$_{AT}$ are shown. Orthogonal cross-sections shown to the right relate to the positions marked in yellow boxes.

We assume that PPK1$_{AT}$-mCherry proteins assemble to higher molecular weight complexes (foci) as it has been shown for PPK1 of *C. crescentus* [Henry and Crosson, 2013]. Presumably, the growing polyP chain is released from PPK1$_{AT}$-mCherry and aggregates to globular polyP granules. Only in the stage of ongoing polyP synthesis, the polyP granule is closely associated with PPK1$_{AT}$-mCherry. Once a polyP granule has been formed, it can now bind other proteins, such as PPK2$_{AT}$, phosins, and others, and at this stage, PPK1$_{AT}$-mCherry can detach from the polyP granule. This "aging phenomenon" would explain why a certain fraction of polyP granules is always located in close association with PPK1$_{AT}$-mCherry foci and another fraction of polyP granules is free of associated PPK1$_{AT}$-mCherry. A similar aging phenomenon has been described for carbonosomes (PHB granules) in *R. eutropha*: for this species, a detachment of eYFP-labeled PHB synthase (PhaC) as well as of its activating protein, PhaM, was observed in time-lapse experiments [Bresan and Jendrossek, 2017].

Dependent on whether *ppk1*$_{AT}$*-mCherry* was expressed from a plasmid or from the native genomic locus, the fluorescence signals were either intense, relatively long (up to 0.5 µm) and slightly curved (online suppl. Fig. s4a), or represented globular foci of relatively low fluorescence intensity, respectively (online suppl. Fig. s4b). We assume that a gene dosis effect is leading to an overexpression of *ppk1-mcherry* in the plasmid system and causes the elongated and intense fluorescence signals in comparison to globular foci of low intensity by genomic *ppk1*$_{AT}$*-mCherry* expression from the own promoter. The polyP granules were generally located in close proximity to the PPK1$_{AT}$-mCherry signals but did not co-localize with them or were located at the opposite cell pole, the OP, independent of PPK1$_{AT}$-mCherry. Interestingly, in those cells that harbored two polyP granules, only one of the polyP granules was associated with a PPK1$_{AT}$-mCherry signal at the GP, while the other was "free" of PPK1$_{AT}$-mCherry and was located at the OP. Figure 2c, d shows a statistical analysis of the distances of polyP granules from the position of the PPK1$_{AT}$-mCherry signals. It is evident that about half of the polyP granules were closely located to the GP-localized PPK1$_{AT}$-mCherry signal, while the other half of the polyP granules were free of a PPK1$_{AT}$-mCherry signal and were located near the opposite cell pole, the OP. PolyP granules were visualized either by co-expression of *eyfp-ppk2*$_{AT}$ (Fig. 2c) or by DAPI staining (Fig. 2d).

The close association of the PPK1$_{AT}$-mCherry signals with polyP granules was investigated at higher resolution by imaging the cells with three-dimensional structured illumination microscopy (3D-SIM). Unfortunately, the fluorescence intensity of the genome-integrated *ppk1*$_{AT}$*-mcherry* gene product was too low to conduct 3D-SIM.

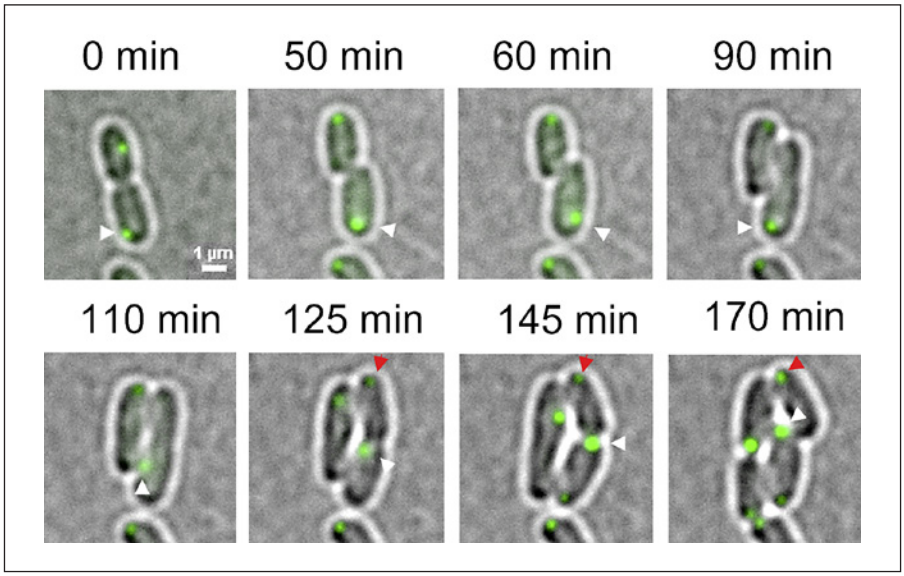

Fig. 4. Migration of polyP granules in *A. tumefaciens*. Snapshots of a time-lapse experiment of *A. tumefaciens* harboring pBBR1MCS2-*eyfp-ppk2*$_{AT}$ at times as indicated are shown. Migration of eYFP-PPK2$_{AT}$ foci (polyP granules) and de novo formation of new eYFP-PPK2$_{AT}$ foci are indicated by white and red arrows, respectively.

We, therefore, show the results of plasmid-derived overexpressed *ppk1*$_{AT}$*-mcherry*. As shown in Figure 3, simultaneous co-expression of *ppk1*$_{AT}$*-mCherry* and *eyfp-ppk2*$_{AT}$ again resulted in fluorescence signals that were close to each other but did not overlap: eYFP-PPK2$_{AT}$ formed spherical, halo-like signals (in *x-y* direction) around unstained ("black") regions resembling the core of polyP granules. This result suggests that eYFP-PPK2$_{AT}$ molecules form a protein layer on the surface of polyP granules but are unlikely to reside inside of the granules. PPK1$_{AT}$-mCherry produced nonspherical but longish and bent fluorescence signals suggesting that PPK1$_{AT}$ is attached to one side of the eYFP-PPK2$_{AT}$-foci.

PolyP Granules Can Migrate from the Old Pole to the Upcoming New Pole during Cell Cycle

A. tumefaciens cells grow asymmetrically at the GP and, after cell division, the former GP becomes an OP, while the new poles of the daughter cells become the new GPs [Grangeon et al., 2015]. To find out when and where new polyP granules are formed, *A. tumefaciens* cells expressing *eyfp-ppk2*$_{AT}$ (to monitor the position of polyP granules without the use of toxic DAPI) were grown in liquid culture (lysogeny broth [LB]) and on LB-agar pads in time-lapse experiments. The presence of the plasmid harboring the *eyfp-ppk2*$_{AT}$ fusion had no detectable impact on growth of the cells (online suppl. Fig. s5). Most cells of an exponentially growing culture had one eYFP-PPK2$_{AT}$ focus that co-localized with DAPI-stained polyP granules as described above (online suppl. Fig. s1b). The same observation was made for cells at the beginning of a time-lapse experiment (Fig. 4, movie 1, https://bit.ly/37fet4o): the two adjacent cells both harbored one eYFP-PPK2$_{AT}$ focus each representing one polyP granule. Analysis of the cells shown in the next time frames indicated that the eYFP-PPK2$_{AT}$ foci of both cells were located at the OPs as evident from growth at the opposite cell ends (GPs). Remarkably, after ≈90 min of growth, the eYFP-PPK2$_{AT}$ focus, i.e., the polyP granule, of one cell (the lower cell in Fig. 4, movie 1) began to migrate to the direction of the GP. Shortly after the onset of the migration of the polyP granule/eYFP-PPK2$_{AT}$ focus, cell invagination at mid-cell became detectable and indicated that the cell was in the process of cell division. Roughly at the time when the migrating eYFP-PPK$_{AT}$ focus had reached the (former) mid-cell position, cell division was completed. The eYFP-PPK2$_{AT}$ focus was now located at the new pole (GP) of one daughter cell. In addition, two new (weakly fluorescent) eYFP-PPK2$_{AT}$ foci appeared shortly before septum formation was completed: one at the GP and one at the OP. After cell division, the upper daughter cell had one eYFP-PPK2$_{AT}$ focus at the former GP (now OP) and the lower daughter cell had two eYFP-PPK2$_{AT}$ foci, one at each cell pole. A similar process was observed in the other cell (the upper cell in Fig. 4, movie 1, https://bit.ly/37fet4o), in which the process of polyP granule/eYFP-PPK2$_{AT}$ movement and cell division started ≈15 min later. A statistical analysis of cells (n = 54) showed that the polyP granules of only approximately one-third of the cells (29%) showed a directional migration, while

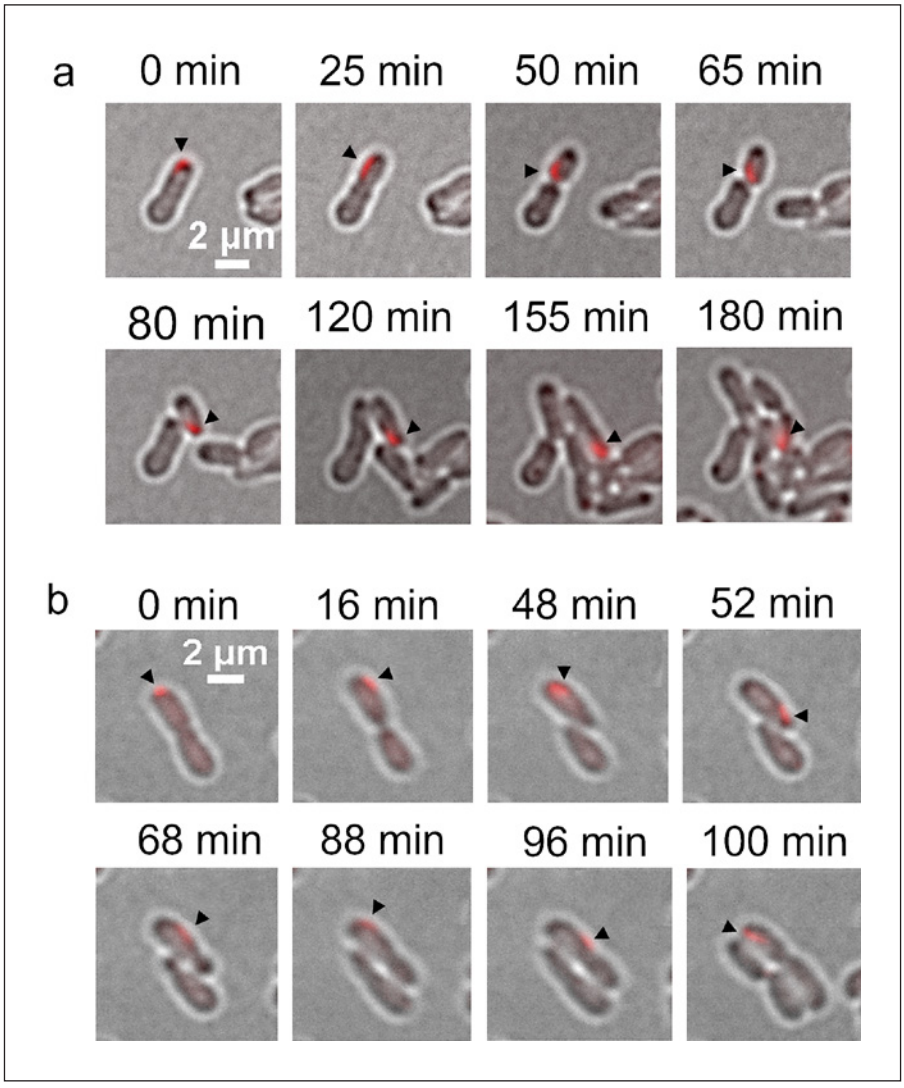

Fig. 5. Migration of $PPK1_{AT}$-mCherry foci in *A. tumefaciens*. Snapshots of a time-lapse experiment of wild-type *A. tumefaciens* harboring pBBR1MCS2-*ppk1*$_{AT}$-*mCherry* (**a**) and of *Δppk1*$_{AT}$*Δppk2*$_{AT}$*A. tumefaciens* harboring pBBR1MCS2-*ppk1(H450A)*$_{AT}$-*mCherry* (**b**) at times as indicated are shown.

the polyP granules of the other cells (71%) did not substantially move or were formed de novo. Similar findings were obtained in several repetitions of these experiments.

$PPK1_{AT}$ of A. tumefaciens Is Involved in polyP Migration

$PPK2_{AT}$ of *A. tumefaciens* is a soluble protein distributed in the cytoplasm in the absence of polyP granules as revealed by a homogeneous fluorescence of eYFP-$PPK2_{AT}$ in a Δ*ppk1* Δ*ppk2* background (online suppl. Fig. s1d). $PPK2_{AT}$ is, therefore, unlikely to be involved in or responsible for the movement or subcellular positioning of polyP granules. To test whether the migration of polyP granules could depend on $PPK1_{AT}$, we followed the localization of $PPK1_{AT}$-mCherry foci in *A. tumefaciens* by time-lapse microscopy. As shown in Figure 5a and movie 2 (https://bit.ly/37fvIlS), $PPK1_{AT}$-mCherry foci were able to migrate from the OP to the GP. To test whether the migration of $PPK1_{AT}$ depended on the presence of polyP granules, we followed the migration of the inactive $PPK1(H450A)_{AT}$-mCherry variant in a polyP-free background (*Δppk1*$_{AT}$, *Δppk2*$_{AT}$*A. tumefaciens*). Interestingly, $PPK1(H450A)_{AT}$-mCherry was also able to migrate. However, the orientation of migration was not restricted to the direction from the OP to the GP, but also the reverse migration of $PPK1(H450A)_{AT}$-mCherry foci from the GP to the OP was detected (Fig. 5b and movie 3, https://bit.ly/2V5RBlp). We conclude that a migration of $PPK1(H450A)_{AT}$-mCherry foci between the cell poles does not depend on the presence of polyP granules. It

seems that an active form of $PPK1_{AT}$ ($PPK1_{AT}$-mCherry) or a wild-type background is necessary for the correct direction of migration from the OP to the GP. This finding is in agreement with the more or less randomly localized $PPK1(H450A)_{AT}$-mCherry foci in a polyP-deficient background (Fig. 2b, orange dots) and the nonrandom localization of active $PPK1_{AT}$ in close association with polyP at the GP (Fig. 2a, black dots). Our result suggests that the presence of polyP is not necessary for migration of $PPK1_{AT}$, but that polyP or other not yet identified molecules are necessary for a correct direction of the migration. The finding that only about one-third of polyP granules is migrating might be explained by a detachment of $PPK1_{AT}$ from polyP granules ("aging" phenomenon, see above): if (only) $PPK1_{AT}$ is responsible for migration, as a consequence, a $PPK1_{AT}$-released polyP granule cannot migrate anymore. The reason, however, why the unidirectional migration from the OP to the GP requires an active form of $PPK1_{AT}$ remains unclear. Perhaps, the polyP-associated CHAD motif containing phosin PptA (Atu4492) or another, not yet identified, polyP granule-attached protein is involved in the coordination of the migration process. We have no evidence (blast analysis) of the presence of related positioning systems for organelle-like structures, such as the McdAB-related carboxysome positioning system in cyanobacteria [MacCready et al., 2018], the PhaM- or PhaF-related proteins in carbonosome-forming bacteria [Galan et al., 2011; Pfeiffer et al., 2011], or the actin-related cytoskeleton-like proteins (MamK/MamJ) in magnetotactic bacteria [Uebe and Schüler, 2016], that might be present in *A. tumefaciens* and could be involved in positioning of polyP granules.

Migration of PPK1a of R. eutropha in A. tumefaciens

To test whether the movement of polyP-associated $PPK1_{AT}$ in *A. tumefaciens* is a specific feature of $PPK1_{AT}$, we expressed *eyfp-ppk1a* of *R. eutropha*, a beta-proteobacterial species in a polyP-free background ($\Delta ppk1_{AT}$, $\Delta ppk2_{AT}$) of *A. tumefaciens* and performed time-lapse studies. PPK1a of *R. eutropha* is responsible for polyP formation in *R. eutropha*; however, polyP granules in *R. eutropha* are located in the nucleoid region and do not migrate during the cell cycle [Beeby et al., 2012; Tumlirsch et al., 2015]. The expression of $eyfp\text{-}ppk1a_{RE}$ in $\Delta ppk1_{AT}$, $\Delta ppk2_{AT}$*A. tumefaciens* restored the formation of polyP granules, but eYFP-$PPK1a_{RE}$ did not colocalize with polyP and formed foci distinct from DAPI-polyP foci as shown in online supplementary Figure s6. Migration of eYFP-$PPK1a_{RE}$ foci was clearly detectable in time-lapse experiments (movie 4, https://bit.ly/3ii0Jft). eYFP-$PPK1a_{RE}$ foci migrated to the GP of the cell. Immediately after cell division, the eYFP-$PPK1a_{RE}$ foci turned back, now moving to the new GP of the daughter cell. Remarkably, the migration of eYFP-$PPK1a_{RE}$ foci appeared to be more rapid than the migration of polyP granules with attached eYFP-$PPK2_{AT}$. These results indicated that the signal to migrate or the signal to bind to a moving molecule is also present in $PPK1a_{RE}$ of *R. eutropha* and does not depend on a co-localized polyP granule. This is somehow unexpected since polyP granules and/or eYFP-$PPK1a_{RE}$ did not show an active movement in *R. eutropha* [unpubl. observation]. We assume that $PPK1_{AT}$ in *A. tumefaciens* interacts with and/or binds to an unknown mobile molecule and that this interaction also functions with $PPK1a_{RE}$ of *R. eutropha*. The primary amino acid sequences of $PPK1_{AT}$ and $PPK1a_{RE}$ share an identity/similarity of 41/58%, respectively. The reason why movement of eYFP-$PPK1a_{RE}$ was more rapid in comparison to $PPK1_{AT}$ might be the early release of the $PPK1a_{RE}$ enzyme from a freshly formed polyP granule in contrast to a much longer association of $PPK1_{AT}$ with polyP. The complex of $PPK1_{AT}$ with polyP has a much higher mass and higher diameter and this might explain the slower movement of eYFP-$PPK1_{AT}$ foci compared to $PPK1a_{RE}$.

Movement of polyP Granules in the Presence of Mitomycin C

What could be the driving force for the $PPK1_{AT}$ movement? The amino acid sequences of $PPK1_{AT}$ and $PPK1a_{RE}$ do not contain known motifs for nucleotide binding such as Walker A/B motifs that could be responsible for providing the energy for migration. We assume that $PPK1_{AT}$ is not a migrating protein per se but is able to bind to another protein or molecule that is moving during the cell cycle and, thus, could explain the movement of $PPK1_{AT}$ and/or $PPK1_{AT}$ with associated polyP. The genome of each cell must replicate and segregate during cell division (for recent reviews on DNA segregation systems see [Gogou et al., 2021; Hu et al., 2021]), and this process includes an active movement of the daughter chromosome(s) to the upcoming daughter cell. We, therefore, hypothesized that $PPK1_{AT}$ could interact with and bind to DNA, thus explaining the observed movement shortly before cell division. To test this hypothesis, we followed the movement of polyP granules that were "stained" with eYFP-$PPK2_{AT}$ in *A. tumefaciens* cells in the presence of mitomycin C (movie 5, https://bit.ly/3C64jAZ). Mitomycin C interacts with DNA and covalently connects the two DNA strand. As a consequence, DNA replication is blocked and, in turn, the cells stop cell division, leading

to the formation of dramatically elongated and often branched cells. Protein biosynthesis and other metabolic reactions are not affected by mitomycin C. In some of our experiments, the *A. tumefaciens* circular chromosome was labeled via expression of a *parB$_{AT}$-mcherry* fusion. When such cells were grown in the presence of 2 µg/mL mitomycin C, the originally rod-shaped short cells turned into long and branched filaments that could still elongate but did not divide anymore. As shown in movie 6 (https://bit.ly/3fjbJaA), the large, branched cell harbored two visible ParB$_{AT}$-mCherry foci that did not, however, migrate during the experiment. They remained more or less at the same position in the middle of the long filament. Analogous experiments in the absence of mitomycin C clearly showed the formation of a ParB$_{AT}$-mCherry focus that divided into two foci, one of which rapidly migrated to the other cell pole before cell division, similar to what has been shown by others previously [Robalino-Espinosa et al., 2020]. This indicated that the concentration of 2 µg/mL of mitomycin C is suited to inhibit cell division and segregation of the circular chromosome but is below lethal levels. When the position of polyP-attached eYFP-PPK2$_{AT}$ foci granules was followed, a back and forth movement of the two eYFP-PPK2$_{AT}$ foci at each end of the approximately 14-µm-long filament by up to 2–4 µm towards the center of the filament and backwards was observed. Apparently, some movement or oscillation of polyP granules was still possible, but unidirectional migration was clearly disturbed. Since the ParB$_{AT}$-mCherry foci did not migrate in the presence of mitomycin C, it is unlikely that polyP granules are attached to the circular chromosome in the neighborhood of parS-bound ParB-mCherry. We cannot, however, exclude that PPK1$_{AT}$ is bound elsewhere, to the linear chromosome or to one of the two plasmids of *A. tumefaciens*.

Directed Movement of polyP Depends on Pole Integrity

Due to the polar growth mode of *A. tumefaciens,* the direction of growth alternates after each cell division [Brown et al., 2012]. As a consequence, the GP of a cell turns into an OP after cell division. This implies that the two poles are differently organized. Indeed, several GP- and OP-specific proteins have been identified in *A. tumefaciens* and in other α-proteobacteria in the last decade. PopZ and PodJ, for example, are specific for the GP and the OP, respectively [Grangeon et al., 2015]. They do not migrate but appear and/or disappear at the respective poles dependent on the cell cycle. Cells without PodJ or without PopZ are disordered in segregation of the circular and the linear chromosome [Robalino-Espinosa et al., 2020]. To test whether mutants impaired in cell pole organization are also impaired in polyP granule migration we followed movement of eYFP-PPK2$_{AT}$-marked polyP granules in PopZ-depleted cells of *A. tumefaciens*. As shown in Figure 6 and movie 7 (https://bit.ly/37cmgjl), depletion of PopZ resulted in the formation of branched cells as previously described [Grangeon et al., 2015; Grangeon et al., 2017; Howell et al., 2017]. In these cells, the eYFP-PPK2$_{AT}$-marked polyP granules did not show a directed migration. Instead, the polyP granules seemed to be located to the area of the cell poles and some of them showed a random oscillation around its position. Apparently, a correctly organized GP is necessary for directed migration of polyP granules.

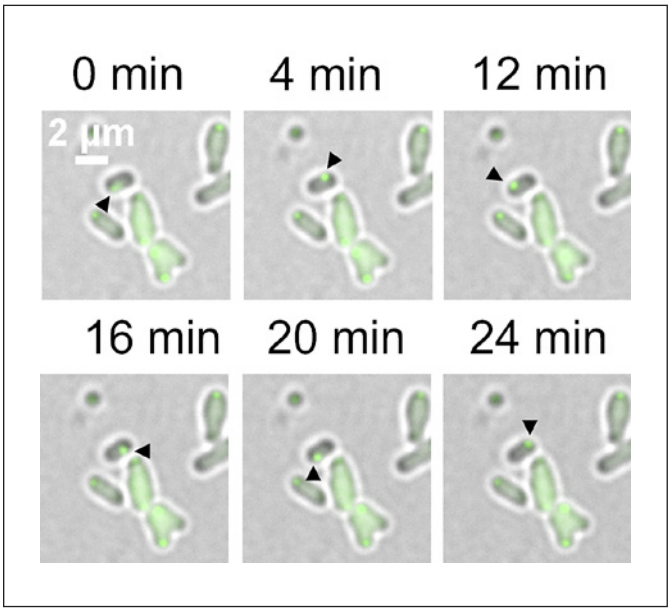

Fig. 6. Migration of polyP granules in PopZ-depleted *A. tumefaciens*. Snapshots of a time-lapse experiment of PopZ-depleted *A. tumefaciens* cells harboring pBBR1MCS2-*eyfp-ppk2$_{AT}$* at times as indicated are shown. The black arrowhead points to an oscillating eYFP-PPK2$_{AT}$ focus.

It is known that segregation of the circular and the linear chromosomes is disordered in PopZ-depleted cells and often results in the formation of mini-cells with absent or incomplete genomes [Grangeon et al., 2017]. We also observed the formation of mini-cells in PopZ-depleted cells. Interestingly, polyP granules in these mini-cells showed a rapid back and forth oscillation between the cell poles of the mini-cells. Further studies including labeling of each genomic element are necessary to obtain deeper insights into the background of PPK1$_{AT}$/polyP move-

Table 1. Strains and plasmids used in this study

Strain/plasmid	Relevant characteristics	Reference
Agrobacterium tumefaciens C58	Wild type, Km^s	[Goodner et al., 2001]
A. tumefaciens Δppk1$_{AT}$*Δppk2*$_{AT}$	Deletion of *ppk1*$_{AT}$ (atu1144) and *ppk2*$_{AT}$ (atu0418)	[Frank and Jendrossek, 2020]
A. tumefaciens ΔpopZ$_{AT}$ depletion	Deletion of *popZ*$_{AT}$ (atu1720) and integration of an IPTG-inducible gene cassette of *popZ*	Pamela Brown, University of Missouri, USA [Ehrle et al., 2017]
Escherichia coli JM109	Cloning strain	DSMZ3423
Ralstonia eutropha H16	Source of *ppk1aRE*	DSMZ428
pTrc200-P*lac*	Broad host range vector, constitutive expression from P*lac*.Sm^r, Spc^r	[Schmidt-Eisenlohr et al., 1999]
pTrc200-P*lac-eyfp-ppk2*	Constitutive expression of *eyfp-ppk2AT*	This study
pBBR1MCS2-P*phaC-eyfp-c1/n1*	Broad host range vector for construction of C (n1)- or N (c1)-terminal gene fusions with *eyfp,* confers Km^r, constitutive expression from P*phaC*	[Pfeiffer et al., 2011]
pBBR1MCS2-P*phaC-mcherry-c1/n1*	Broad host range vector for construction of C (n1)- or N (c1)-terminal gene fusions with *mCherry,* confers Km^r, constitutive expression from P*phaC*	[Pfeiffer et al., 2011]
pBBR1MCS2-P*phaC-popZ*$_{AT}$*-eyfp*	Constitutive expression of *popZ*$_{AT}$*-eyfp*	This study
pBBR1MCS2-P*phaC-eyfp-ppk2*$_{AT}$	Constitutive expression of *eyfp-ppk2*$_{AT}$	[Frank and Jendrossek, 2020]
pBBR1MCS2-P*phaC-mcherry-ppk2*$_{AT}$	Constitutive expression of *mcherry-ppk2*$_{AT}$	This study
pBBR1MCS2-P*phaC-eyfp-pptA*$_{RE}$	Constitutive expression of *eyfp-pptA*(A0104)$_{RE}$	[Tumlirsch and Jendrossek, 2017]
pBBR1MCS2-P*phaC-ppk1*$_{AT}$*-mcherry*	Constitutive expression of *ppk1*$_{AT}$*-mcherry*	[Frank and Jendrossek, 2020]
pBBR1MCS2-P*phaC-ppk1*(H450A)$_{AT}$*-mcherry*	Constitutive expression of *ppk1*(H450A)$_{AT}$*-mcherry*	This study
pBBR1MCS2-P*ppk1-ppk1*(H450A)$_{AT}$*-mcherry*	Constitutive expression from P*ppk1* of *ppk1*(H450A)$_{AT}$*-mcherry*	This study
pBBR1MCS2-P*phaC-eyfp-ppk1a*$_{RE}$	Constitutive expression of *eyfp-ppk1a*(A2437)$_{RE}$	[Tumlirsch et al., 2015]
pBBR1MCS2-P*phaC-parB*$_{AT}$*-mcherry*	Constitutive expression of *parB*(atu2828)$_{AT}$*-mcherry*	This study

Km^s/Km^r, kanamycin sensitivity/resistance; Sm^r/Spc^r, streptomycin/spectinomycin resistance.

ment. Furthermore, the determination of the polyP proteome of *A. tumefaciens* is necessary to identify other, so far unknown, polyP-associated proteins that might be involved in migration of polyP granules. Interestingly, a similar approach in *P. aeruginosa* very recently led to the identification of AlgP as a novel polyP-associated protein that is responsible for equidistant spacing of multiple polyP granules in *P. aeruginosa* [Chawla et al., 2021].

Materials and Methods

Bacterial Strains, Plasmids and Culture Conditions

Bacterial strains and plasmids used in this study are listed in Table 1. *A. tumefaciens* C58 strains were cultivated in LB (88 rpm agitation)-medium supplemented with the appropriate antibiotics at 30°C or 28°C. The *A. tumefaciens ΔpopZ* depletion strain was pre-cultured in the presence of IPTG to induce expression of the *popZ* gene. For depletion experiments, the pre-culture was centrifuged and the cell pellet was resuspended in fresh LB-medium without IPTG.

Construction of Gene Fusions and of Gene Deletions

The PCR-assisted construction of in frame gene fusions of *ppk* genes with *mCherry* or *eyfp* and transformation of *A. tumefaciens* cells was performed as previously described [Lenz and Friedrich, 1998; Frank and Jendrossek, 2020]. For construction of gene deletions, the *sacB*-containing pLO3 suicide vector was used [Frank and Jendrossek, 2020]. An analogous procedure was applied for the formation of genomic gene fusions and exchange of the parental gene by the gene fusion. Each constructed plasmid/strain was verified by DNA sequencing of the total region of the modified DNA.

Microscopic Methods

Fluorescence microscopy was done as described in detail elsewhere [Hildenbrand et al., 2019; Frank and Jendrossek, 2020].

3-µL portions of cells were immobilized on agarose pads (1% (wt/vol) in phosphate buffered saline) and covered with a coverslip. For time-lapse experiments, 3 µL of the respective cell suspension were added to the bottom surface of an LB-Agar pads (1% (wt/vol) in LB-medium) and – after drying for 15–30 s – were put into a nunc glass base dish (12 mm). The borders of the agar pad were sealed with ≈150 µL of liquid (50°C) LB-agar. Drying of the agar pad during the time-lapse experiment was reduced by adding water-soaked filter paper into the nunc glass base dish. Care was taken that the filter paper did not touch the agar pad. The closed dishes were incubated at 28°C or 30°C in an incubation chamber and imaged every 4–5 min for up to 12 h.

Structured Illumination Microscopy (3D-SIM)

3D-SIM (striped illumination at 3 angles and 5 phases) was performed using an Eclipse Ti2-E N-SIM E microscope (Nikon) equipped with a CFI SR Apo TIRF AC 100×H NA1.49 oil objective lens, LU-N3-SIM laser unit (Nikon) (488/561/640 nm wavelength lasers; emission filters: 525/50, 605/70, 700/75 nm), and an Orca Flash4.0 LT Plus sCMOS camera (Hamamatsu). Sample preparation employing precision cover glasses (0.17 mm thickness, No. 1.5H, Marienfeld) and calibration of the motorized objective correction collar and SIM grating focus using fluorescent beads with a diameter of 100 nm (T-7279 TetraSpeck microspheres) were performed at 24°C as described previously [Pfeiffer et al., 2019]. To correct for color shift between channels during 3D-SIM image reconstruction, the system was calibrated using T-7279 TetraSpeck microspheres and the N-SIM color registration. 3D-SIM imaging was performed using exposure times in the range of 20–80 ms at 40–60% laser power. *z*-series were acquired at a total thickness of 1.50–2.64 µm with 50–120 nm *z*-step spacing. Image reconstruction was performed in NIS-Elements 5.11 (Nikon) using either the "slice reconstruction" algorithm (illumination modulation contrast: auto; high resolution noise suppression: 0.1; blur suppression: 0.01) or the "stack reconstruction" algorithm for *z*-stack data (illumination modulation contrast: auto; high resolution noise suppression: 0.1).

Evaluation of Microscopical Pictures

Images were processed using Fiji/ImageJ software [Schindelin et al., 2012] in combination with ObjectJ [Vischer et al., 2015] to determine cell length and position of fluorescent foci (scale 15.5px/µm).

Acknowledgements

We gratefully acknowledge the support by P. Brown/University of Missouri, Columbia, MO, USA) for providing the *A. tumefaciens ΔpopZ* depletion strain and P. Zambrysky (University of California, Berkeley, CA, USA) for advice in time-lapse experiments. We also thank F. Narberhaus (University of Bochum, Bochum, Germany) for support in *A. tumefaciens* techniques and helpful discussions.

Statement of Ethics

Ethical approval was not required for this study (no experiments with humans or animals).

Conflict of Interest Statement

The authors have no conflicts of interest to declare.

Funding Sources

This work was supported by a grant of the Deutsche Forschungsgemeinschaft (DFG) to D.J. and RTG1708.

Author Contributions

C.F. performed most of the experiments, prepared the figures, and wrote parts of the manuscript. D.P. performed 3D-SIM experiments. M.A. supported the project by advice and assistance on how to manipulate *A. tumefaciens*. D.J. designed the study and wrote most parts of the manuscript. All authors evaluated the data and read the manuscript.

Data Availability Statement

All data generated or analyzed during this study are included in this article and in its online supplementary material files. Links to electronic files of time-lapse movies are embedded in the text and are additionally provided in the online supplementary material files.

References

Beeby M, Cho M, Stubbe J, Jensen GJ. Growth and localization of polyhydroxybutyrate granules in *Ralstonia eutropha*. J Bacteriol. 2012 Mar; 194:1092–9.

Bresan S, Jendrossek D. New insights in PhaM-PhaC-mediated localization of PHB granules in *Ralstonia eutropha* H16. Appl Environ Microbiol. 2017 Apr 7. AEM.00505–17.

Bowman GR, Comolli LR, Zhu J, Eckart M, Koenig M, Downing KH, et al. A polymeric protein anchors the chromosomal origin/ParB complex at a bacterial cell pole. Cell. 2008 Sep 19;134:945–55.

Brown PJ, de Pedro MA, Kysela DT, Van der Henst C, Kim J, De Bolle X, et al. Polar growth in the Alphaproteobacterial order Rhizobiales. Proc Natl Acad Sci U S A. 2012 Jan 31;109: 1697–701.

Chawla R, Klupt S, Patsalo V, Williamson JR, Racki LR. The Histone H1-like protein AlgP facilitates even spacing of polyphosphate granules in *Pseudomonas aeruginosa*. bioRxiv. 2021 Sep. http://dx.doi.org/10.1101/2021.08.24.457604.

Ebersbach G, Briegel A, Jensen GJ, Jacobs-Wagner C. A self-associating protein critical for chromosome attachment, division, and polar organization in *Caulobacter*. Cell. 2008 Sep 19;134:956–68.

Ehrle HM, Guidry JT, Iacovetto R, Salisbury AK, Sandidge DJ, Bowman GR. Polar organizing protein PopZ Is required for chromosome segregation in *Agrobacterium tumefaciens*. J Bacteriol. 2017 Sep 1;199:e00111–17.

Frank C, Jendrossek D. Acidocalcisomes and polyphosphate granules are different subcellular structures in *Agrobacterium tumefaciens*. Appl Environ Microbiol. 2020 Feb 14; 86:e02759–19.

Frank C, Teleki A, Jendrossek D. Characterization of *Agrobacterium tumefaciens* PPKs reveals the formation of oligophosphorylated products up to nucleoside nona-phosphates. Appl Microbiol Biotechnol. 2020 Oct 6;104:9683–92.

Galan B, Dinjaski N, Maestro B, de Eugenio LI, Escapa IF, Sanz JM, et al. Nucleoid-associated PhaF phasin drives intracellular location and segregation of polyhydroxyalkanoate granules in *Pseudomonas putida* KT2442. Mol Microbiol. 2011 Jan;79:402–18.

Gogou C, Japaridze A, Dekker C. Mechanisms for chromosome segregation in bacteria. Front Microbiol. 2021;12:685687.

Goodner B, Hinkle G, Gattung S, Miller N, Blanchard M, Qurollo B, et al. Genome sequence of the plant pathogen and biotechnology agent *Agrobacterium tumefaciens* C58. Science. 2001 Dec 14;294:2323–8.

Grangeon R, Zupan JR, Anderson-Furgeson J, Zambryski PC. PopZ identifies the new pole, and PodJ identifies the old pole during polar growth in *Agrobacterium tumefaciens*. Proc Natl Acad Sci U S A. 2015 Sep 15;112:11666–71.

Grangeon R, Zupan J, Jeon Y, Zambryski PC. Loss of PopZ At activity in *Agrobacterium tumefaciens* by deletion or depletion leads to multiple growth poles, minicells, and growth defects. MBio. 2017 Nov 14;8:e01881–17.

Harold FM. Inorganic polyphosphates in biology: structure, metabolism, and function. Bacteriol Rev. 1966 Dec;30:772–94.

Henry JT, Crosson S. Chromosome replication and segregation govern the biogenesis and inheritance of inorganic polyphosphate granules. Mol Biol Cell. 2013;24:3177–86.

Hildenbrand JC, Reinhardt S, Jendrossek D. Formation of an organic-inorganic biopolymer: polyhydroxybutyrate-polyphosphate. Biomacromolecules. 2019 May 7. acs.biomac.9b00208.

Howell M, Aliashkevich A, Salisbury AK, Cava F, Bowman GR, Brown PJB. Absence of the polar organizing protein PopZ results in reduced and asymmetric cell division in *Agrobacterium tumefaciens*. J Bacteriol. 2017 Sep 1;199:e00101–17.

Hu L, Rech J, Bouet JY, Liu J. Spatial control over near-critical-point operation ensures fidelity of ParABS-mediated DNA partition. Biophys J. 2021 Sep 21;120(18):3911–24.

Jendrossek D. Polyphosphate granules and acidocalcisomes. In: Jendrossek D, editor. Bacterial Organelles and Organelle-Like Inclusions. Microbiology Monographs. Springer; 2020. p. 1–17.

Kornberg A, Rao NN, Ault-Riché D. Inorganic polyphosphate: A molecule of many functions. Annu Rev Biochem. 1999;68:89–125.

Lenz O, Friedrich B. A novel multicomponent regulatory system mediates H2 sensing in *Alcaligenes eutrophus*. Proc Natl Acad Sci U S A. 1998;95:12474–9.

Lorenzo-Orts L, Hohmann U, Zhu J, Hothorn M. Molecular characterization of CHAD domains as inorganic polyphosphate-binding modules. Life Sci Alliance. 2019 Jun;2: e201900385.

MacCready JS, Hakim P, Young EJ, Hu L, Liu J, Osteryoung KW, et al. Protein gradients on the nucleoid position the carbon-fixing organelles of cyanobacteria. Elife. 2018 Dec 6;7: 850.

MacCready JS, Basalla JL, Vecchiarelli AG. Origin and evolution of carboxysome positioning systems in cyanobacteria. Mol Biol Evol. 2020 May 1;37:1434–51.

Meyer A. Orientirende Untersuchungen über Verbreitung Morphologie und Chemie des Volutins. Bot Zft. 1904;62:113–52.

Murata K, Hagiwara S, Kimori Y, Kaneko Y. Ultrastructure of compacted DNA in cyanobacteria by high-voltage cryo-electron tomography. Sci Rep. 2016 Oct 12;6:34934–8.

Pallerla SR, Knebel S, Polen T, Klauth P, Hollender J, Wendisch VF, et al. Formation of volutin granules in *Corynebacterium glutamicum*. FEMS Microbiol Lett. 2005 Feb 1;243:133–40.

Pfeiffer D, Wahl A, Jendrossek D. Identification of a multifunctional protein, PhaM, that determines number, surface to volume ratio, subcellular localization and distribution to daughter cells of poly(3-hydroxybutyrate), PHB, granules in *Ralstonia eutropha* H16. Mol Microbiol. 2011 Nov;82:936–51.

Pfeiffer D, Toro-Nahuelpan M, Bramkamp M, Plitzko JM, Schüler D. The polar organizing protein PopZ is fundamental for proper cell division and segregation of cellular content in *Magnetospirillum gryphiswaldense*. MBio. 2019 Mar 12;10:7.

Racki LR, Tocheva EI, Dieterle MG, Sullivan MC, Jensen GJ, Newman DK. Polyphosphate granule biogenesis is temporally and functionally tied to cell cycle exit during starvation in *Pseudomonas aeruginosa*. Proc Natl Acad Sci U S A. 2017 Mar 6;114:E2440–E2449.

Rao NN, Gómez-García MR, Kornberg A. Inorganic polyphosphate: essential for growth and survival. Annu Rev Biochem. 2009;78:605–47.

Robalino-Espinosa JS, Zupan JR, Chavez-Arroyo A, Zambryski P. Segregation of four *Agrobacterium tumefaciens* replicons during polar growth: PopZ and PodJ control segregation of essential replicons. Proc Natl Acad Sci U S A. 2020 Oct 6;117:26366.

Schmidt-Eisenlohr H, Domke N, Baron C. TraC of IncN plasmid pKM101 associates with membranes and extracellular high-molecular-weight structures in Escherichia coli. J Bacteriol. 1999 Sep;181:5563–71.

Seufferheld M, Vieira MC, Ruiz FA, Rodrigues CO, Moreno SN, Docampo R. Identification of organelles in bacteria similar to acidocalcisomes of unicellular eukaryotes. J Biol Chem. 2003;278:29971–8.

Schindelin J, Arganda-Carreras I, Frise E, Kaynig V, Longair M, Pietzsch T, et al. Fiji: an open-source platform for biological-image analysis. Nat Methods. 2012 Jun 28;9:676–82.

Takade A, Umeda A, Misumi T, Sawae Y, Amako K. Accumulation of phosphate-containing granules in the nucleoid area of *Pseudomonas aeruginosa*. Microbiol Immunol. 1991;35: 367–74.

Toro-Nahuelpan M, Müller FD, Klumpp S, Plitzko JM, Bramkamp M, Schüler D. Segregation of prokaryotic magnetosomes organelles is driven by treadmilling of a dynamic actin-like MamK filament. BMC Biol. 2016;14:88.

Tumlirsch T, Sznajder A, Jendrossek D. Formation of polyphosphate by polyphosphate kinases and its relationship to poly(3-hydroxybutyrate) accumulation in *Ralstonia eutropha* strain H16. Appl Environ Microbiol. 2015 Dec;81:8277–93.

Tumlirsch T, Jendrossek D. Proteins with CHADs (Conserved Histidine α-Helical Domains) are attached to polyphosphate granules in vivo and constitute a novel family of polyphosphate-associated proteins (phosins). Appl Environ Microbiol. 2017 Apr 1;83:e03399–16–4.

Uebe R, Schüler D. Magnetosome biogenesis in magnetotactic bacteria. Nat Rev Microbiol. 2016 Sep 13;14:621–37.

Vischer NOE, Verheul J, Postma M, van den Berg van Saparoea B, Galli E, Natale P, et al. Cell age dependent concentration of *Escherichia coli* divisome proteins analyzed with ImageJ and ObjectJ. Front Microbiol. 2015;6:586.

Voelz H, Voelz U, Ortigoza RO. The "polyphosphate overplus" phenomenon in *Myxococcus xanthus* and its influence on the architecture of the cell. Arch Mikrobiol. 1966 May 9;53: 371–88.

Werten S, Rustmeier NH, Gemmer M, Virolle MJ, Hinrichs W. Structural and biochemical analysis of a phosin from *Streptomyces chartreusis* reveals a combined polyphosphate- and metal-binding fold. FEBS Lett. 2019 Jun 10;593: 2019. 1873–3468.13476–2029

Zupan JR, Cameron TA, Anderson-Furgeson J, Zambryski PC. Dynamic FtsA and FtsZ localization and outer membrane alterations during polar growth and cell division in *Agrobacterium tumefaciens*. Proc Natl Acad Sci U S A. 2013 May 28;110:9060–5.